Challenging Glass 5 – Conference on Architectural and Structural Applications of Glass
Belis, Bos & Louter (Eds.), Ghent University, June 2016.

ISBN 978-90-825-2680-6

The Role of Restraints on the Buckling Response of Glass Shear Walls

C. Bedon & C. Amadio
DIA, University of Trieste, Italy, chiara.bedon@dia.units.it

In current practice, glass shear walls are frequently used to cover wide surfaces in facades. There, a multitude of restraints can be found, depending on specific aesthetic, architectural and structural requirements. Typical practical examples can in fact take the form of linear adhesive joints, metal frames or mechanical point fixings, etc. From a practical point of view, as a result, it is clear that compared to idealized boundary conditions the actual restraints should be properly taken into account. In this research paper, the shear buckling response of glass shear walls is assessed by means of Finite-Element (FE) simulations and analytical methods. The role of (i) linear adhesive joints, (ii) metal frames with interposed adhesive joints or (iii) point mechanical connectors on the theoretical buckling resistance of these panels is first assessed (e.g. in the form of fundamental buckling shapes and Euler's critical loads). Analytical fitting curves of general applicability are proposed, so that classical formulations derived from shear buckling theories could be used. Subsequently, the actual shear buckling resistance is also assessed, e.g. by taking into account the effects of possible initial geometrical imperfections, damage in glass or in the adopted restraints. This goal is achieved by means of accurate but computationally efficient FE models able to reproduce (via mechanical connectors, *surface-to-surface* interactions, etc.) the desired mechanical effect of restraints, as well as any possible local damage in them. As shown, rather close agreement is found with a past normalized buckling curve in use for ideally simply supported glass shear walls. It is thus expected, in view of further investigations and full-scale experimental validation, that the current research outcomes could provide a useful theoretical background for the implementation of standardized buckling design methods.

Keywords: Glass Shear Walls, Shear Buckling, Design Standardization, Finite-Element Numerical Modelling

1. Introduction and state-of-the-art

Glass panels are widely used in modern buildings as structural elements. Frequent applications in façades, for example, involve the use of glass panels spanning from floor to floor (e.g. restrained at the level of foundation and roof) able to ensure lightness, transparency and energy efficiency to wide surfaces and interiors. Often, the same glass panels are used for architectural and comfort requirements, but especially in the form of 'glass walls' able to ensure stabilization and stiffening contributions to entire buildings and structural systems, in the form of structural panels able to carry on compressive, bending and shear forces due to the external loads (e.g. uniform pressures acting orthogonally to the plane of glass, in-plane compressive loads deriving from the adjacent structural background, or in-plane shear loads due to pressures acting along a direction parallel to the same glass panels' surface). As a result, their design and calculation strictly depends on a complex structural interaction between the glass panels themselves and their connections to the substructures, namely consisting in glued bonded connections, adhesive joints, special metal fasteners, steel or aluminum frames, as well as timber framing systems. In this sense, it is clear that an appropriate estimation of the effect of special restraints (compared to ideal boundary conditions) on the overall structural performance of these glass walls is mandatory. In doing so, based on the typical high slenderness ratios which characterize structural glass components in general, careful consideration should be paid especially for buckling phenomena due to a single main action as well as a combination of multiple loads.

Over the past years, several researchers investigated the structural performance of shear glass walls and assemblies under in-plane quasi-static as well as dynamic loads, such in the case of seismic events. The major number of these past research projects has been dedicated to the development and validation of novel design concepts for the connection systems, as well as to the implementation and calibration of standardized design methods of practical use for glass shear walls under ordinary loads. Huveners et al. (2007) experimentally investigated the structural behavior of glass panels subjected to in-plane shear loads and circumferentially glued to metal frameworks. The structural interaction between glass panels and adhesively bonded steel frames has been also studied in (Richter et al 2014). In (Memari et al. 2004; Behr 2006), the dynamic behavior of full-scale curtain wall mock-ups was experimentally investigated were carried out to assess the seismic vulnerability and flexibility of glass façade panels under in-plane earthquake loads. Antolinc et al. (2014) also investigated, by means of full-scale shake-table experiments, the seismic capacity of glass walls interacting with timber frames.

Mocibob (2008) focused on the experimental and Finite-Element (FE) numerical investigation of the structural behavior of laminated glass panels under in-plane shear loads, with specific attention for their shear buckling performance. In that work, careful consideration was paid for glass walls point supported to the substructure by

means of bolted metal fasteners, as well as for glass panels linearly supported at the top and bottom edges only via partially rigid, flexible, linear adhesive joints. Wellershoff (2006) also assessed via experiments and FE simulations the buckling response of glass panels under in-plane shear and continuously, linearly supported along the four edges. Analytical and FE studies were proposed in (Bedon and Amadio 2012) for the assessment of the buckling response and resistance of glass panels ideally simply supported along the four edges, under the action of in-plane shear loads. Based on a further validation of a simplified equivalent thickness approach, the study was then extended in (Amadio and Bedon 2013) to laminated glass panels composed of two (or three) glass sheets and one (or two) shear flexible viscoelastic PVB films. In that case, the calibration of a Eurocode-based design curve to experimental test results of literature, FE simulations and analytical calculations was also proposed as a rational buckling design procedure for the examined loading and boundary conditions. The mentioned standardized design method, due to its general validity and simplicity of application, is currently implemented in technical documents for structural glass elements (e.g. (CNR-DT 210/2013)). Its actual limitation, however, is represented by the assumption of ideal restraint conditions only (e.g. fully rigid, continuous simply supports along the four edges).

In this work, the buckling response of glass panels subjected to in-plane shear loads is further investigated by means of extended FE parametric simulations (ABAQUS/Standard) and analytical methods. Careful consideration is paid, compared to the earlier research contributions, to the overall effect of specific boundary conditions of practical use, e.g. (i) structural adhesive linear joints, (ii) supporting metal frames with interposed adhesives, (iii) mechanical point fixings. Throughout exploratory FE parametric studies, the theoretical shear buckling response is first assessed, e.g. in terms of fundamental buckling shape and Euler's critical load. As shown, as also in accordance with Mocibob (2008), the (i) to (iii) restraint typologies can strongly modify the shear behavior and ultimate resistance of the examined shear walls, compared to classical simply supported conditions. This latter assumption, specifically, would lead to marked overestimation of the actual resistance, for almost the cases of practical interest. For a given glass shear wall and restraint configuration, moreover, the overall shear buckling behavior strictly depends on a combination of multiple aspects, e.g. the geometrical and mechanical properties of the glass panel alone as well as of the restraints (e.g. adhesive stiffness and thickness, out-of-plane bending stiffness of the metal frame, number and position of point mechanical connectors). As a result, an appropriate estimation and description of all the related global / local effects is mandatory for safe design purposes. In this paper, buckling coefficients numerically derived from linear bifurcation FE simulations are proposed, together with appropriate analytical fitting curves of general applicability, so that for a given geometry and (i) to (iii) restraint typology, the corresponding Euler's critical load could be calculated based on classical formulations derived from shear buckling theories (Timoshenko and Gere 1961). Based on extended nonlinear incremental FE analyses, the validity of the buckling design curve presented in (Amadio and Bedon 2013) for ideally, continuously supported glass panels under in-plane shear is also properly highlighted. As shown, due to the appropriate estimation of the effect of restraints on the corresponding shear buckling response, a rather good agreement is found, hence suggesting the extension of the same buckling design approach to various boundary conditions of practical interest. A practical case study is also proposed, in conclusion, to further emphasize the effect of restraints on the actual shear buckling response of a given glass panel. Certainly, extended full-scale experimental investigations could provide a further substantial validation of the presented analytical methods. In this sense, it is expected that the current research outcomes could provide a strong theoretical background for the examined structural typologies.

2. Classical theoretical background *vs* practical glass shear walls applications

2.1. Monolithic panels with ideal restraints

Often, buckling design methods proposed in literature for structural elements composed of various construction materials are strictly derived from classical analytical formulations for plates, beams, columns, under the hypotheses of ideal mechanical material behavior as well as boundary and loading conditions. In doing so, the estimation of the corresponding Euler's critical load represent a first – although not fully exhaustive – information related to the expected buckling performance for the structural element object of study.

When assessing the shear buckling response of a monolithic, fully isotropic panel subjected to in-plane shear loads, for example, with reference to Figure 1a, analytical calculations are usually performed by taking into account classical formulations derived from literature (Timoshenko and Gere 1961), that is by assuming that (i) the material has an elastic, homogeneous, isotropic behavior; (ii) the panel is initially perfectly flat and its thickness is small, compared to the global dimensions; (iii) the strains due to deflection in the middle surface are negligible, compared to strains due to bending; and (iv) deformations are such that straight lines initially normal to the middle surface remain straight and normal. The corresponding Euler's critical shear load is given by:

$$V_{cr,0}^{(E)} = \frac{\pi^2 D}{b^2} k_\tau \tag{1}$$

where $D = Ebt^3 / 12(1-\nu^2)$ denotes the bending stiffness of the panel; b, H are the global dimensions; t the nominal thickness; E the Young's modulus; ν and Poisson' ratio. In the same Equation, k_τ is the buckling coefficient depending on the assigned boundary conditions and the aspect ratio $\alpha = H/b$. For panels with fully simply supported edges ('ss-ss'), k_τ is (Timoshenko and Gere 1961):

$$k_\tau = \begin{cases} 4.00 + \dfrac{5.34}{\alpha^2} & \alpha \le 1 \\ 5.34 + \dfrac{4.00}{\alpha^2} & \alpha > 1 \end{cases} \tag{2}$$

As far as the actual restraints can be rationally assumed to behave as ideal, continuous simply supports or fully clamps, the Euler's critical load given by Eq.(1) can represent a useful and rational estimation of the expected buckling resistance of a given panel under in-plane shear loads V.

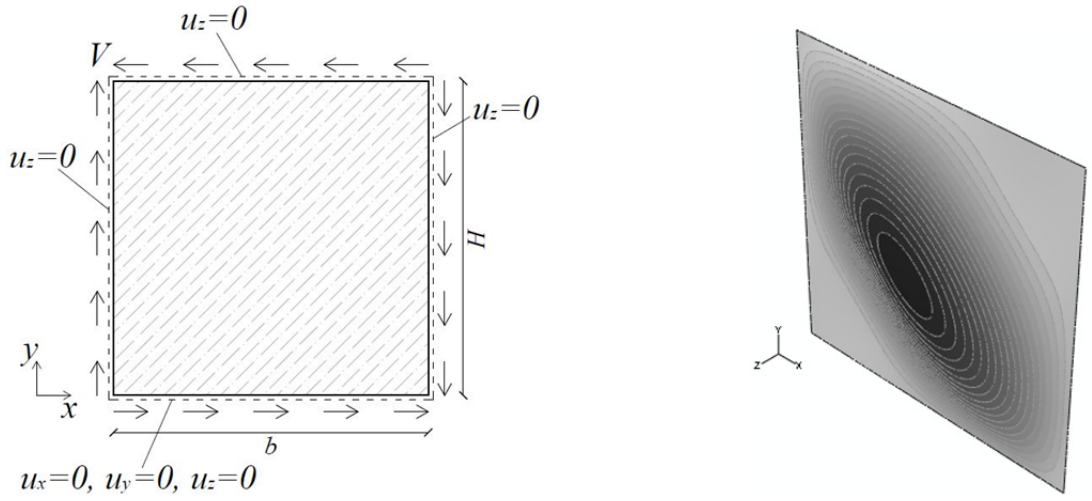

Fig. 1 Theoretical model for a simply supported, isotropic plate under in-plane shear. a) Reference system and b) fundamental deformed shape.

2.2. Common restraints for practical glass shear wall applications

When specific restraints are used in practice, appropriate studies should be carried out, e.g. in the form of detailed but often time consuming FE simulations, so that the effect of these restraints on the global structural response of the examined shear walls could be properly taken into account. In modern building applications, glass shear walls are in fact often supported by means of (i) linear adhesive joints (e.g. Figure 2(a)), (ii) metal frameworks (e.g. Figure 2(b)), (iii) mechanical point fixings (e.g. Figure 2(c)). Especially (i) adhesive joints and (iii) point mechanical connectors are used, due to their capacity to minimize the presence of bracing systems.

In the first case (i), see Figure 2(a), the typical connection takes the form of a two-side adhesive joint applied along the top and bottom edges only of glass, with vertical edges full unrestrained. Additional small steel supports, working as unilateral compressive restraints only, are used to transmit the compressive reaction forces from the glass panel to the structural background (Mocibob 2008). Further small gaskets and spacers (see for example the cross-sectional detail of Figure 2) are used to kept fix the glass panel in the desired position, hence to allow possible rotations within the restraining system itself.

The same design concept was extended in (Amadio and Bedon 2015), by introducing metal bracing components (e.g. mullions with a given out-of-plane bending stiffness) able to provide further restraint against possible deformations of the panel (see Figure 2(b)). In this latter case, the shear buckling response of the examined panels results from a combination of multiple geometrical and mechanical aspects, e.g. depending on the features of the glass panel only, the metal frame and the interposed adhesive joints.

The last examined restraint condition (iii), finally, is characterized by the presence of mechanical point-fixings only. The detail of Figure 2(c) represents the typical mechanical point-fixing for glass applications, namely consisting in a stainless steel head and a soft layer gasket (e.g. a polymeric ('POM') spacer) or a small mortar layer (Mocibob 2008)) able to improve the distribution and propagation of maximum tensile stresses near the glass hole edges. Such point-fixing connectors typically provide transnational and rotational restraints to the supported glass panels, hence

their actual working mechanism should be properly taken into account. Through the current exploratory investigation, the number and position of these point connectors is originally set equal to n_b= 4, with ϕ= 42mm the glass hole diameter and d= 100mm the distance from each hole center to the panel edges (see also Mocibob 2008), while subsequently the configurations with n_b= 6 or 8 point connectors vertically aligned onto two columns, with $100 \leq d \leq 150$mm, are also investigated (see Section 4.3).

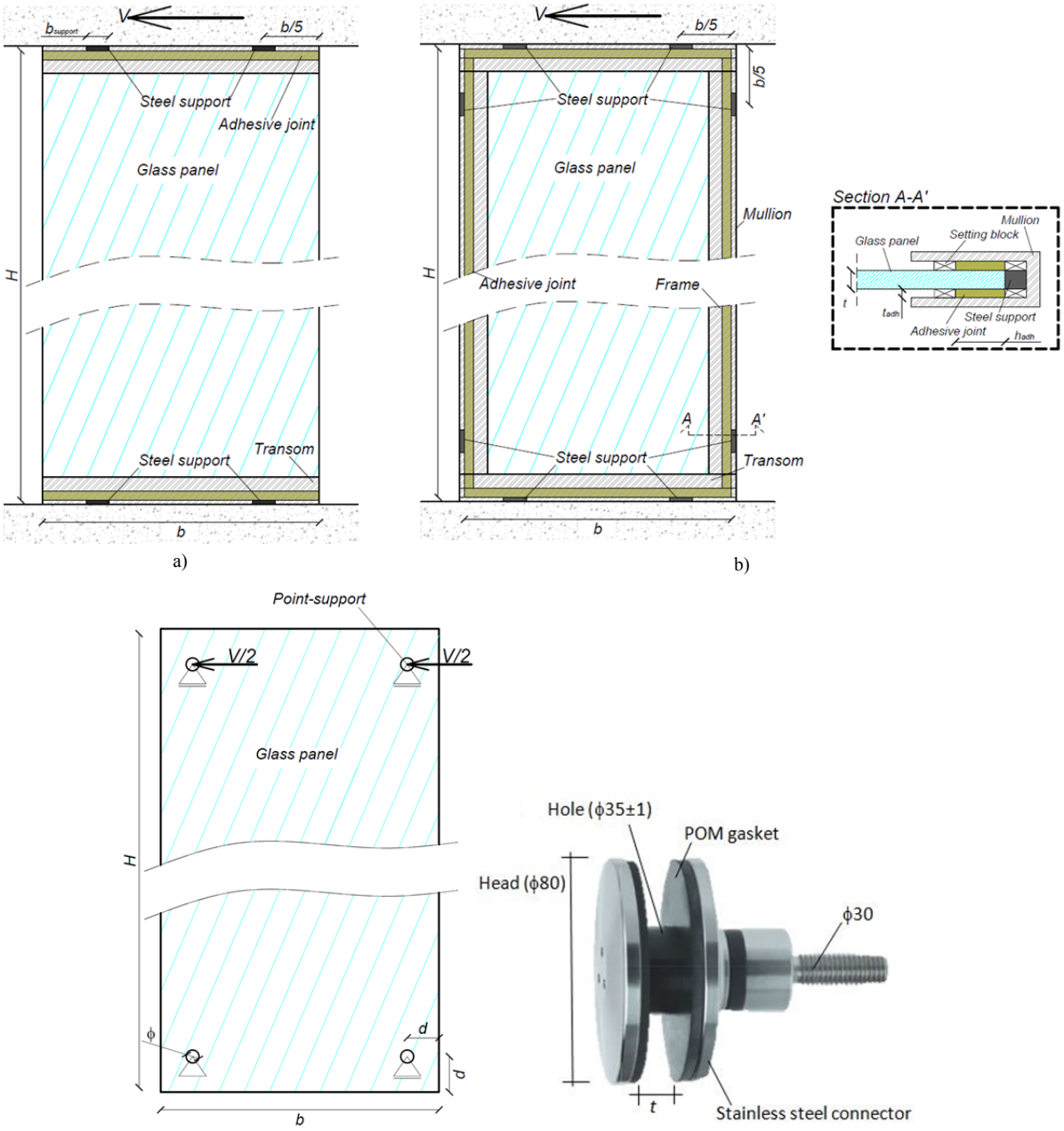

Fig. 2 Reference practical cases for the shear buckling assessment of glass walls. a) Linear adhesive joints, b) metal frame with interposed adhesive joints and b) point mechanical supports.

3. Extended FE numerical study

3.1. General FE modelling approach

The typical FE-model was implemented in the ABAQUS/Standard computer software (Simulia 2010) and consisted of 4-node shell elements composed of glass and characterized by a monolithic thickness t.

FE simulations were in fact carried out both on monolithic and three-layer laminated glass panels. In the latter case, the nominal sandwich cross-section composed of two glass sheets (t_1 and t_2 the thicknesses) and a middle bonding foil (t_{int} the thickness and G_{int} the shear modulus) was approximated in the form of a fully monolithic resisting section fully composed of glass, in which the equivalent thickness $t = t_{eq} = f(t_1, t_2, t_{int}, E, G_{int})$ was calculated as

proposed in (Amadio and Bedon 2013) for three-layer laminated glass panels under in-plane shear loads. For the specific load-time and temperature conditions taken into account through the FE parametric study, the corresponding values of shear modulus G_{int} were carefully estimated, based on master curves available in literature for PVB or SG foils (see for example (Van Duser et a. 1999)). In the implementation of the aforementioned equivalent thickness approach, finally, glass was mechanically described in the form of an indefinitely linear elastic material, with E= 70GPa, ν= 0.23 the Young's modulus and Poisson' ratio respectively (EN 572-2: 2004). In this sense, any possible tensile failure or crushing mechanism was manually checked.

3.2. FE implementation and mechanical characterization of restraints

Careful consideration was given to the geometrical and mechanical description of restraints, e.g. the linear adhesive joints (Figure 2(a)), the metal frames with interposed adhesive joints (Figure 2(b)) and the point mechanical connectors (Figure 2(c)), being these restraints representative of the main influencing parameter for the current FE numerical study. The computational accuracy and efficiency of the FE models were ensured by using equivalent axial springs with damage mechanical models, unilateral point connectors and *surface-to-surface* interactions. Figure 3 provides an overview of the main FE modelling assumptions. A detailed description of the FE mechanical calibration of the same restraints, for the (i) to (iii) typologies, can be found in (Bedon and Amadio 2016a), (Amadio and Bedon 2015) and (Bedon and Amadio 2016b) respectively, together to a preliminary FE validation towards experimental results available in literature for small specimens/components.

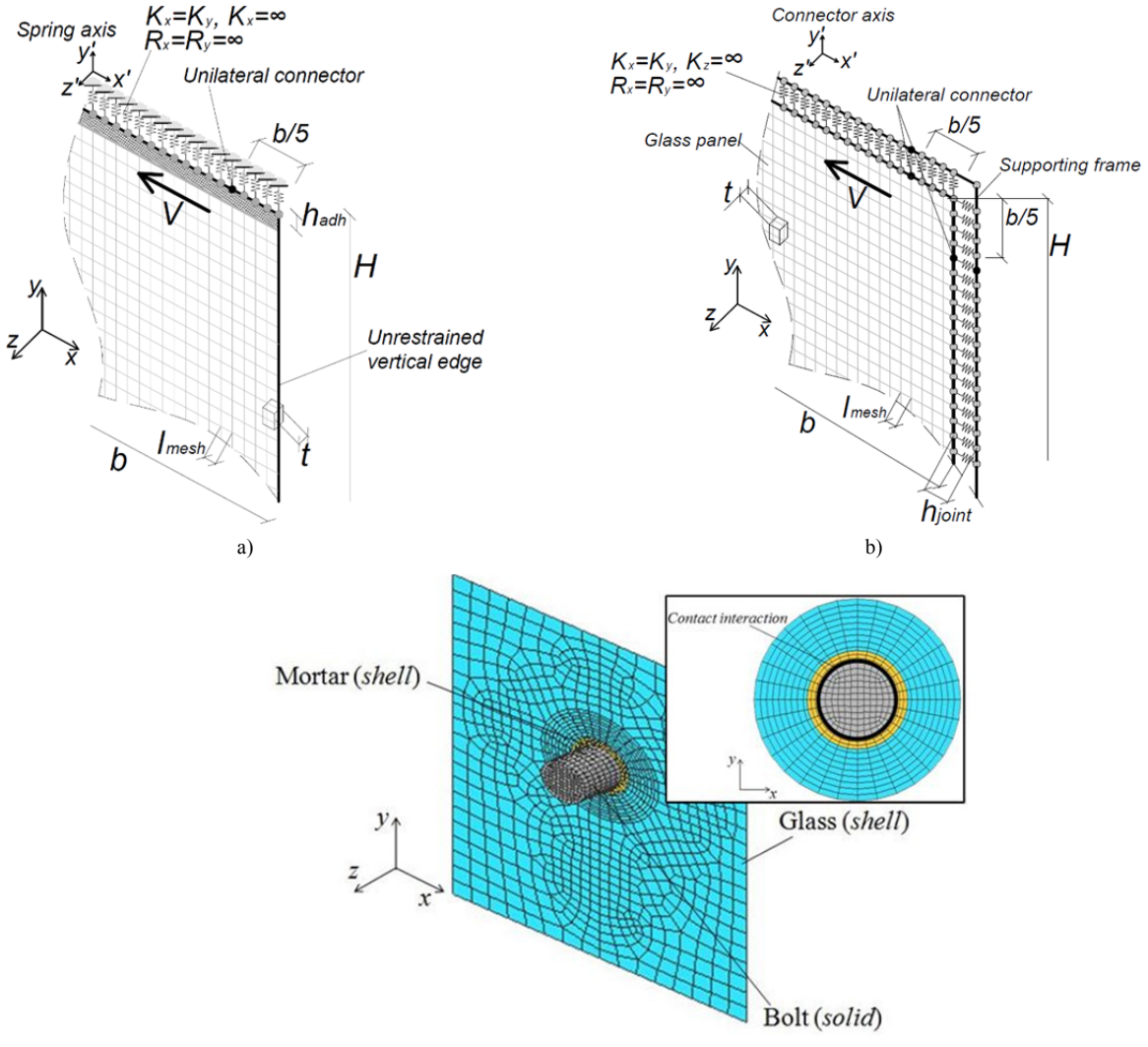

Fig. 3 Overview of the typical FE modelling approach for the implementation of the restraint details in glass shear walls. a) Linear adhesive joints, b) metal frame with interposed adhesive joints and c) mechanical point-fixing connectors.

3.3. FE solving method

Both linear bifurcation analyses (*lba*) and geometrical incremental nonlinear simulations (*inls*) were carried out on the reference geometrical cases discussed above. The same FE mechanical modelling approach was used both for *lba* and *inls* analyses. In the first case (*lba* simulations, see Section 4), qualitative assessment of the role of restraints

was carried out in terms of fundamental buckling shapes and Euler's critical loads. In the latter case (*inls* study, see Section 5), the overall shear buckling response was investigated, with careful consideration for the shape and amplitude of possible initial geometrical imperfections (with H/1000 the minimum recommended amplitude, in absence of more accurate data). Due to the basic assumption of fully linear elastic constitutive law for glass, any possible damage mechanism (both tensile or crushing phenomena) were in fact detected as the first attainment on glass surface of maximum principal stresses exceeding the characteristic tensile and compressive resistances respectively, in accordance with the nominal values derived from product standards (EN 572-2: 2004).

In view of a validation of a past design buckling curve currently implemented in the Italian technical document CNR-DT 210/2013, the ultimate shear buckling resistance was generally detected as the first attainment of possible: (i) tensile cracking in glass, (ii) crushing mechanisms (e.g. in the vicinity of point-fixings and steel supports); (iii) maximum out-of-plane deformations exceeding a pre-fixed value (H/300, in this case, in accordance with (Amadio and Bedon 2013)).

4. Discussion of *lba* FE results and derivation of k_τ fitting curves

A first exploratory investigation was carried out in the form of parametric linear bifurcation analyses (*lba*), for all the examined restraint typologies. Based on Eq.(1), k_τ was in fact reasonably derived as:

$$k_\tau = \left(V_{cr,0}^{(E)}\right)_{lba} \frac{b^2}{\pi^2 D} = \left(V_{cr,0}^{(E)}\right)_{lba} \frac{b \cdot 12\left(1-\nu^2\right)}{\pi^2 E t^3}. \tag{3}$$

4.1. Linear adhesive joints

Variations in the geometrical/ mechanical properties of the glass panels (e.g. overall dimensions and cross-section) and the adhesive (e.g. Young's modulus E_{adh} and cross-sectional dimensions $t_{adh} \times h_{adh}$) were taken into account. Some of the so obtained FE results are proposed in Figure 4(a), where numerically estimated k_τ coefficients (ABAQUS-*lba*) are proposed as a function of the panels aspect ratio α, while the difference between the collected plots is given by the stiffness K_{adh} of the adhesive connection, where

$$K_{adh} = n_{adh} \cdot \left(\frac{E_{adh}}{2 \cdot \left(1+\nu_{adh}\right)} \frac{h_{adh}}{t_{adh}} \right), \tag{4}$$

in [MPa], n_{adh}= 2 for adhesive layers applied on both the glass panel faces, ν_{adh}= 0.49 for the Poisson's ratio, while h_{adh} and t_{adh} the cross-sectional dimensions respectively (see the details provided in Figures 2(a)-(b)).

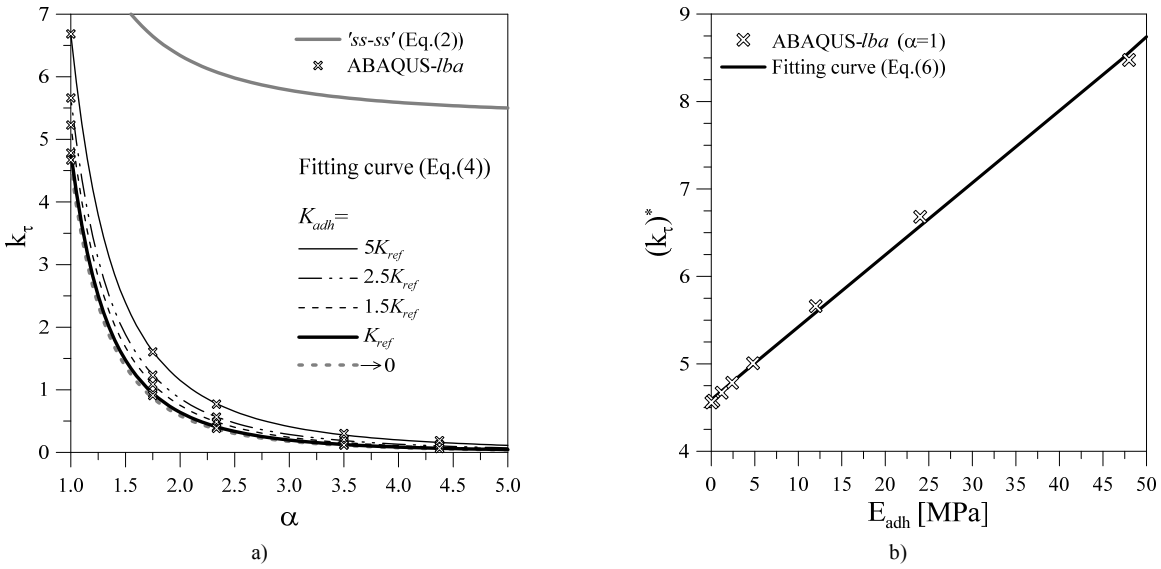

Fig. 4 FE numerically derived and analytical fitting curves for linear adhesively restrained glass shear walls. a) k_τ buckling coefficients and b) FE-analytical comparisons.

In Figure 4(a), in particular, the FE data and analytical fitting plots are expressed as a function of a 'reference' joint stiffness K_{adh}= K_{ref}. This K_{ref} value was calculated, in accordance with (Mocibob 2008), by means of Eq.(4) with n_{adh}= 2, E_{adh}= 2.4MPa and t_{adh} = 9.5mm × h_{adh}= 40mm the nominal dimensions of a single adhesive layer (see Figure 2(a)). By assuming $(k_\tau)^*$ as the value of the (k_τ, α) curves for α= 1, it can be seen from Figure 4(a) that the collected

plots have almost a regular trend (e.g. at least as far as K_{adh} do not exceeds 5 times the reference value, in this FE parametric study), generally expressed by fitting curves in the form:

$$k_\tau = \frac{(k_\tau)^*}{\alpha^y} \approx \frac{(k_\tau)^*}{\alpha^3} \tag{5}$$

which well agrees with findings results proposed in (Mocibob 2008), and

$$(k_\tau)^* = \frac{K_{adh}}{c_1} + c_2 \tag{6}$$

with K_{adh} given by Eq.(4), c_1= 12.2 MPa and c_2= 4.6.

For all the tested panel, as also in accordance with (Mocibob 2008), the corresponding fundamental buckling shape was characterized by large out-of-plane deflections for the fully unrestrained vertical edges of glass, e.g. Figure 6(a).

4.2. Metal frames

As far as supporting mullions were added with increasingly out-of-bending stiffness to provide a certain bracing effect to the vertical edges of the examined glass panels (e.g. Figure 2(b)), a shear buckling response rather sensitive to a multitude of combined aspects was observed (e.g. geometrical / mechanical properties of the glass panel only, the supporting metal frame, the interposed adhesive joints).

In any case, all the collected *lba* FE data highlighted a general agreement with an analytical fitting curve defined in the form (see Figure 5a):

$$k_\tau = \frac{c_3}{\alpha^{c_4}} \tag{7}$$

with

$$c_3 = X + 0.39 \cdot \ln(R_{EI}) \tag{8}$$

$$c_4 = \frac{1}{0.04 \cdot R_{EI} + 0.365} \tag{9}$$

and

$$R_{EI} = \frac{2EI_m}{EI_g} \tag{10}$$

a bending stiffness ratio, where EI_m is the out-of-plane bending stiffness of a single supporting metal mullion and

$$EI_g = E_g \cdot \frac{bt^3}{12} \tag{11}$$

the bending stiffness of the glass panel only, while

$$X = c_5 \cdot K_{adh} + 6.67 \tag{12}$$

and c_5= 0.03 MPa^{-1} define the c_3 constant of Eq.(8). Figure 5(b) shows a parametric comparison between the FE predicted and analytically fitted k_τ buckling coefficients.

In terms of qualitative effect due to bracing mullions characterized by variable out-of-plane bending stiffness, a transition between the limit conditions of (i) glass panel with fully unrestrained vertical edges (e.g. Figure 6(a)) and (ii) glass panels with fully rigidly restrained vertical edges (e.g. Figure 6(c)) was also noticed, with typical

fundamental buckling shapes agreeing (for the range of geometrical / mechanical properties of major interest in structural glass applications) with Figure 6(b).

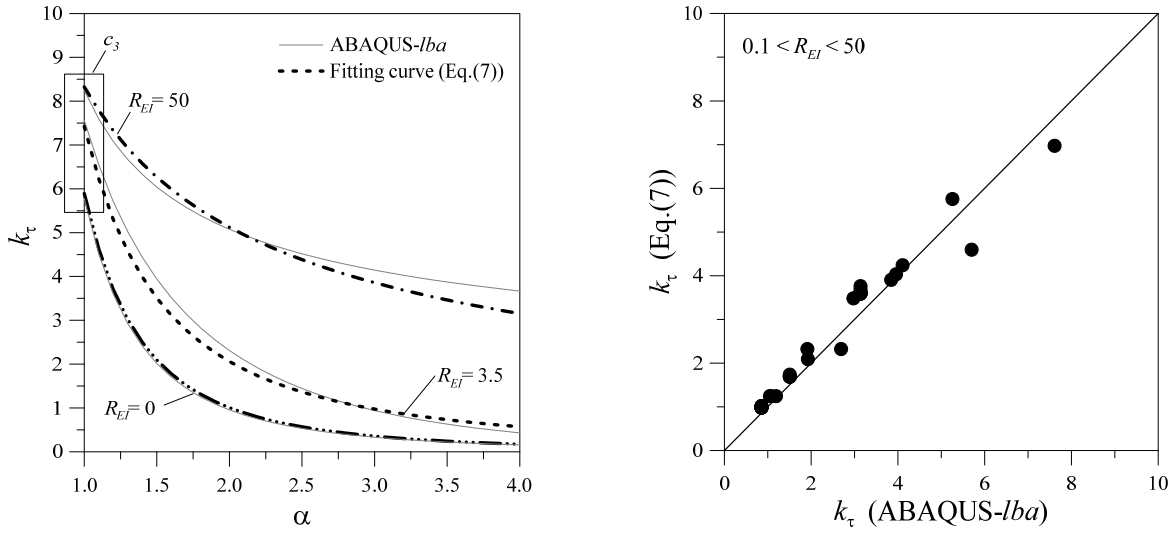

a) b)

Fig. 5 FE numerically derived and analytical fitting curves for frame supported glass shear walls. a) k_τ buckling coefficients and b) FE-analytical comparisons.

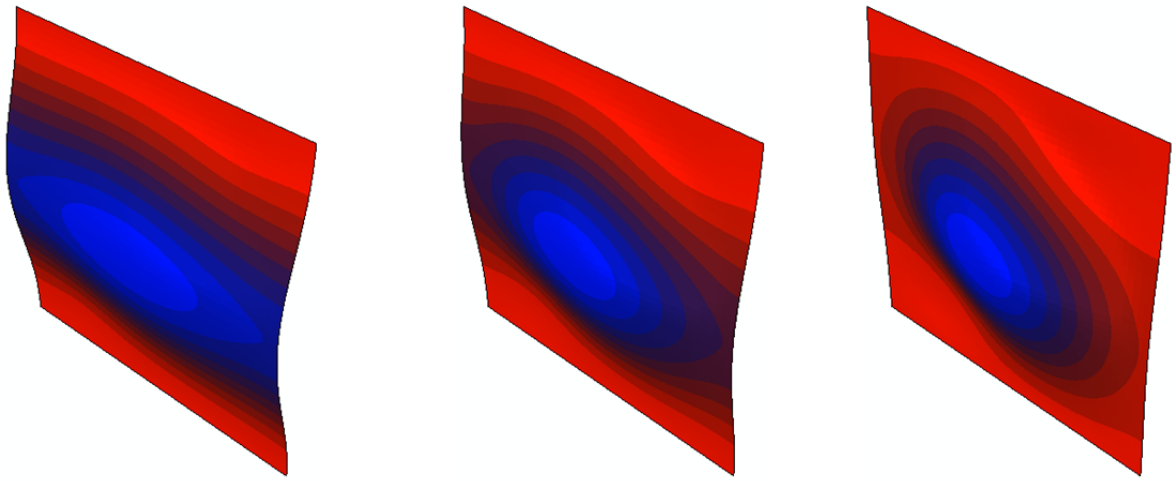

a) R_{EI}= 0 b) R_{EI}= 5 c) R_{EI}= 50

Fig. 6 FE fundamental buckling shapes for glass shear walls supported by metal frames with variable out-of-plane bending stiffness (ABAQUS/Standard).

4.3. Mechanical point-fixings

In the case of point-supported glass panels under in-plane shear, the *lba* study was performed by taking into account several geometrical configurations, e.g. overall dimensions and cross-section of the tested glass panels, in accordance with Figure 2(c), as well as various configurations of point-fixing restraints (e.g. d= 100, 120, 150 mm the distance of the holes center from the edges, or n_b= 4, 6 and 8 the total number of connectors).

In general, the performed *lba* studies highlighted a rather negligible sensitivity of theoretical buckling resistance / buckling coefficients k_τ to the position of the point-connectors (e.g. the distance d), and an almost close agreement (for the n_b= 4, 6, 8 examined configurations) with the following analytical fitting curve:

$$k_\tau = \frac{c_6}{\alpha^{c_7}} \tag{13}$$

being

$$c_6 = 1.88 \cdot n_b - 3.46 \tag{14}$$

and $c_7 = 2$.

An almost linear correlation was in fact found, for a given geometry, between the number of point restraints and the corresponding Euler's critical load / k_τ coefficient (see Figure 7). In this sense, compared to the n_b= 4 reference case, the additional point supports (n_b= 6 or 8) worked in fact as intermediate rigid restraints able to progressively reduce the effective buckling length of the panel, see Figures 7(b) and 8. In terms of theoretical buckling resistance, e.g. k_τ coefficient, the presence of multiple point-fixings able to provide both translation and rotational restraints typically resulted in an overall strength markedly lower than the ideal '*ss-ss*' configuration (Figure 7(a)). Local over-strengthening effects, at the same time, were found for very short panels only (e.g. $\alpha < \approx 1.5$, Figure 7(a)) with $n_b >$ 4. Since these local effects were limited to a range of aspect ratios α is typically associated in practice to n_b= 4 point connectors, the validity of the proposed analytical fitting curves was properly limited to $\alpha \geq 1$ and $\alpha \geq 1.5$ for glass panels with n_b= 4 or $n_b > 4$ respectively.

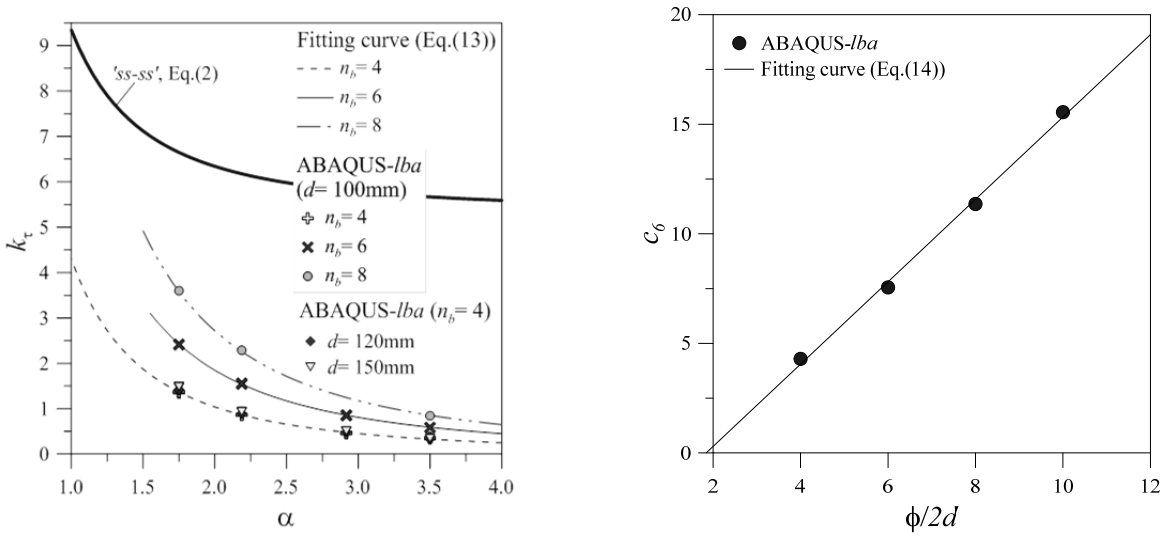

a) b)

Fig. 7 FE numerically derived (ABAQUS/Standard) and analytical fitting curves for point supported glass shear walls. a) k_τ buckling coefficients and b) c_6 fitting curve.

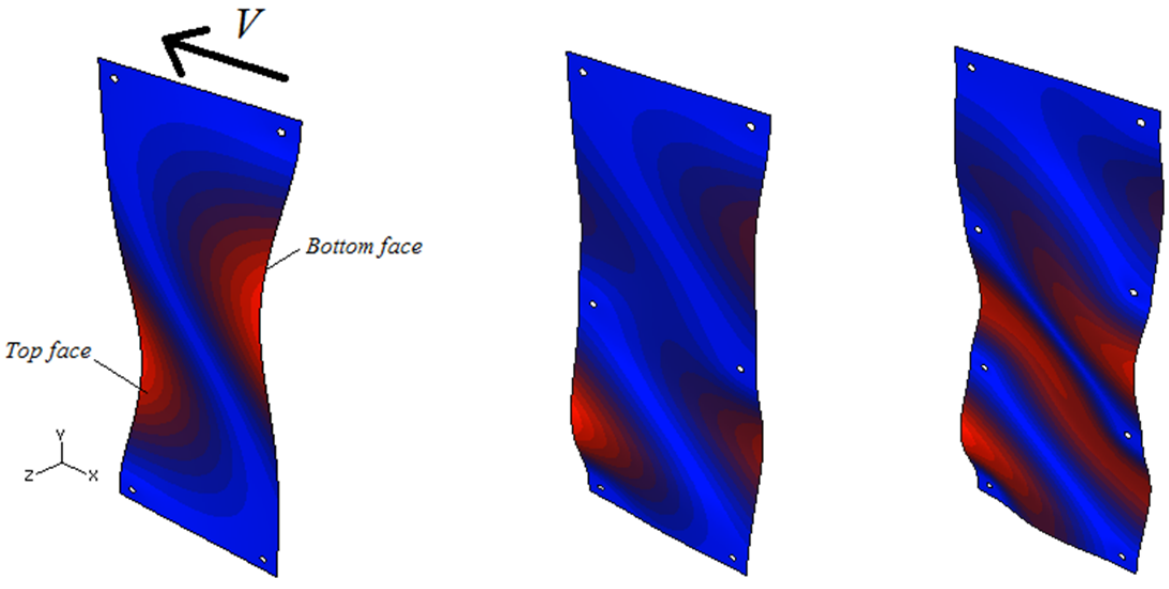

a) n_b= 4 b) n_b= 6 c) n_b= 8

Fig. 8 FE fundamental buckling shapes for glass shear walls with mechanical point connectors (ABAQUS/Standard).

5. Generalized design buckling curve

As a conclusive step of this exploratory investigation, *inls* parametric studies were carried out on a multitude of shear glass panels with various geometrical properties and restraints typologies, according to Section 3. As far as the *lba* simulations provide an almost qualitative assessment of the expected shear buckling response for the examined panels, *lba* analyses are not able to take into account the effects of several aspects, such as geometrical defects, mechanical damage phenomena, etc., and more detailed, geometrical nonlinear analyses (*inls*) are mandatory.

5.1. Validation of existing method

In this research contribution, the *inls* parametric simulations were carried out to assess and validate the accuracy of the standardized design method proposed in (Amadio and Bedon 2013) for ideally simply supported glass plates under in-plane shear. In that case, a Eurocode-based design curve was in fact calibrated, so that the shear buckling verification of a given shear glass panel could be carried out as:

$$V = V_{Ed} \le V_{b,Rd} = \chi \frac{\tau_{Rk} \cdot A^*}{\gamma_M} \tag{15}$$

with $\tau_{Rk} = \sigma_{Rk}$ the nominal tensile resistance of glass (EN 572-2: 2004), $A^* = bt^*$ the resisting cross-sectional surface of glass only (e.g. total glass thickness t^*, both in the case of monolithic or laminated sections), $\gamma_M = 1.4$ a material partial safety factor (Wellershoff 2006) and

$$\chi = \frac{1}{\Phi + \sqrt{\Phi^2 - \overline{\lambda}^2}} \quad \text{for } \chi \le 1 \tag{16}$$

a buckling reduction coefficient, where

$$\Phi = 0.5[1 + \alpha_{imp}(\overline{\lambda} - \alpha_0) + \overline{\lambda}^2] \tag{17}$$

$$\overline{\lambda} = \sqrt{\frac{\tau_{Rk} \cdot A^*}{V_{cr,0}^{(E)}}} \tag{18}$$

the normalized slenderness ratio and $\alpha_{imp} = 0.49$, $\alpha_0 = 0.50$ the imperfection factors calibrated by taking into account an initial geometrical imperfection with $H/1000$ the maximum amplitude.

The parametric FE data collected from the current *inls* study are proposed in Figure 9, in non-dimensional form. There, FE dots are proposed for adhesive / frame supported glass shear walls (Figure 9(a)) and point supported panels (Figure 9(b)) subjected to initial geometrical imperfections derived – for each restraint typology – from preliminary *lba* analyses and scaled up to $H/1000$ the panels height.

The difference between Figures 9(a) and (b) is given by the normalization process for the collected FE data. While in the first case the cross-sectional resisting surface A^* is still represented by the full bt^* glass section, hence:

$$\overline{\lambda} = \overline{\lambda}_1 = \sqrt{\frac{\tau_{Rk} \cdot A^*}{\left(V_{cr,0}^{(E)}\right)_{lba}}} \tag{19}$$

and

$$\chi = \chi_1 = \frac{V_{b,Rd} \cdot \gamma_M}{\tau_{Rk} \cdot A^*}, \tag{20}$$

for the point-supported shear walls the normalization approach was carried out by taking into account the effects due to glass holes, e.g. by calculating the slenderness ratio as:

$$\overline{\lambda} = \overline{\lambda}_2 = \sqrt{\frac{\tau_{Rk} \cdot A_n^* / K_t}{\left(V_{cr,0}^{(E)}\right)_{lba}}} \tag{21}$$

with

$$A_n^* = (2d - \phi) \cdot t^* \tag{22}$$

the reduced resisting area and

$$K_t = 3 - 3.13 \cdot \left(\frac{\phi}{2d}\right) + 3.66 \cdot \left(\frac{\phi}{2d}\right)^2 - 1.53 \cdot \left(\frac{\phi}{2d}\right)^3 \tag{23}$$

the stress concentration factor (Peterson 1953), while the buckling reduction factor was calculated as

$$\chi = \chi_2 = \frac{V_{b,Rd} \cdot \gamma_M}{\left(\frac{\tau_{Rk} \cdot A_n^*}{K_t}\right)}. \tag{24}$$

The so normalized FE data, for both Figures 9(a) and (b), are thus proposed by taking into account several glass types (e.g. annealed, heat strengthened and fully tempered) and their corresponding characteristic tensile resistance values (EN 572-2: 2004). In terms of compressive resistance, conversely, a conventional characteristic limit value of 450MPa was considered (≈10 times the nominal tensile strength of float glass).

As shown, for all the examined mechanical and geometrical configurations, a rather close agreement was found between the FE data and the past standardized design buckling curve. In the case of point supported glass panels only (Figure 9(b)), modified imperfection factors α_0= 0.30 and α_{imp}= 1.40 were also calibrated and proposed for safe estimations (e.g. due to the high sensitivity of this latter configuration to local failure phenomena, as especially emphasized by glass shear walls with n_b= 4). Certainly, further extended investigations and full-scale experimental validations are required. In any case, the current research outcomes suggest the possible generalization of standardized buckling design methods to structural glass panels with variable restraint conditions.

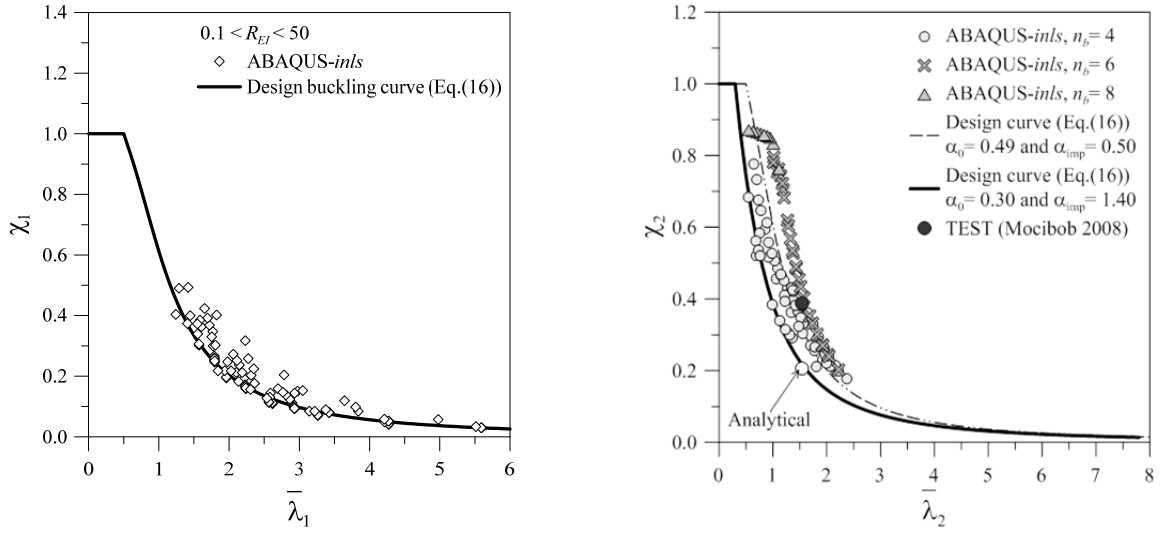

Fig. 9 Assessment of a past normalized design buckling curve (Eq.(16)) for glass shear walls with a) adhesive joints and metal frame with interposed adhesive joints or b) mechanical point-supports (γ_M= 1, for the normalization of ABAQUS-*inls* data).

5.2. Practical calculation example

As a practical example, a glass panel with overall dimensions b= 1m and H= 3m was finally taken into account. Its cross-section was supposed composed of two heat strengthened glass panels, with t_1= t_2= 12mm the nominal thicknesses, bonded together by means of a PVB film (with t_{int}= 1.52mm the thickness). The shear buckling resistance of the so assembled panel was assessed towards the action of a short-term wind pressure with resultant force V_{Ed} acting in the plane of the glass wall itself. For the examined loading condition, a conventional duration of 30 seconds and a reference temperature of 20°C can be taken into account for design purposes (e.g. (CNR-DT 210/2013)), hence G_{int}= 8.06MPa was considered as the corresponding equivalent shear modulus for PVB. Based on (Amadio and Bedon 2013), a fully monolithic, equivalent thickness of 17.42mm was used for the parametric analytical calculations, with t^*= 24mm the total thickness of glass only. For the same geometrical configuration and loading condition, the shear buckling response was in fact investigated by taking into account several boundary conditions, see Table 1.

Table 1: Reference restraint properties for the practical examples collected in Figure 10.

Reference #	Restraint typology	Main features
0	*ss-ss*	Idealized, continuous simply supports along the four edges
1	Adhesive (i)	Adhesive joints along the top/bottom edges only, with t_{adh}= 9.5mm, h_{adh}= 40mm, n_{adh}= 2 and E_{adh}= 1.2MPa, while b/5 is the distance of small steel supports from the corners
2	Adhesive (i)	The same of #1, but E_{adh}= 2.4MPa
3	Adhesive (i)	The same of #1, but h_{adh}= 80mm
4	Frame + adhesive (ii)	Metal frame + adhesive joints, with R_{EI}= 0.5 and adhesive joints characterized as in #1
5	Frame + adhesive (ii)	The same of #4, but R_{EI}= 2
6	Frame + adhesive (ii)	The same of #4, but R_{EI}= 10
7	Frame + adhesive (ii)	The same of #4, but R_{EI}= 50 (fully rigid frame)
8	Point-fixing (iii)	Mechanical point-fixing connectors with d= 100mm, ϕ= 42mm, n_b= 4
9	Point-fixing (iii)	The same of #8, but n_b= 6
10	Point-fixing (iii)	The same of #8; but n_b= 8

The shear buckling parameters (e.g. critical load $V_{b,Rd}$ and normalized slenderness ratio $\overline{\lambda}$) were calculated for the #0 to #10 configurations, based on Eqs.(15) and (18) respectively (with $A^* \equiv A_n^*/K_t$ for the point-supported panels), and compared in non-dimensional form in Figure 10, where:

$$R = \frac{p_{(\#0)}}{p_{(\#i)}}, \quad i = 0,..10 \tag{25}$$

denotes the ratio between each 'p' parameter for the #0 restraint configuration of Table 1, compared to the other #i-cases.

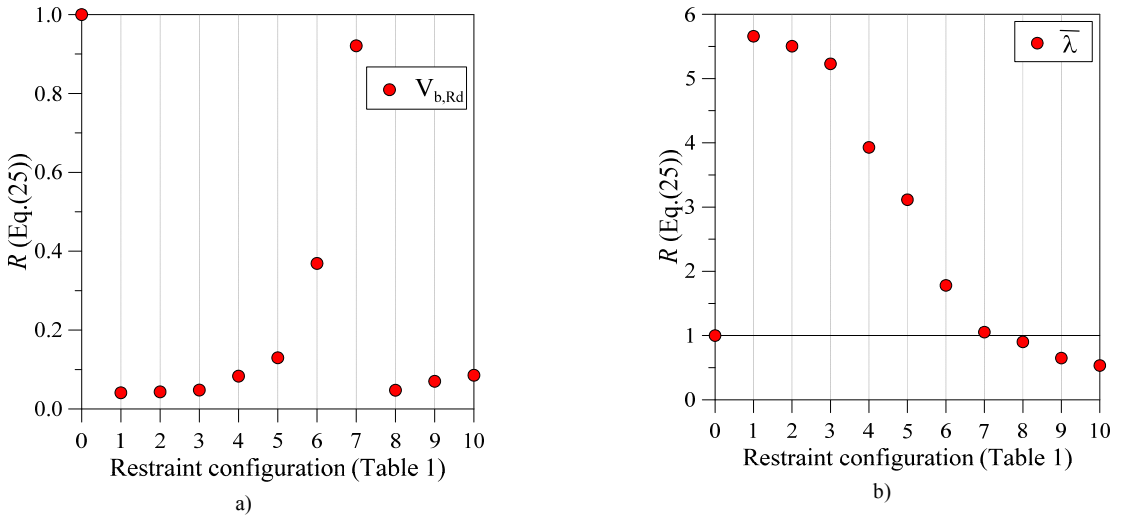

Fig. 10 Analytical comparative shear buckling calculations for a given glass wall geometry with several restraint typologies and subjected to a short term in-plane shear load. a) Design critical buckling load (Eq.(15)) and b) normalized slenderness ratio (Eq.(18)).

As shown in Figure 10, as expected, a marked effect of restraints was found for all the examined configurations. In terms of buckling resistance $V_{b,Rd}$ (Figure 10(a)), the assumption of a conventional '*ss-ss*' reference case would lead to a marked overestimation of the actual design strength, for panels with adhesive (#1 to #3), metal frames (#5, #6) and point-fixing supports (#8 to #10). In most of the cases, the design resistance $V_{b,Rd}$ was in fact found to be in the order of ≈0.1-0.3 times the '*ss-ss*' value.

This effect typically derives from a combination of aspects strictly related to the mechanical and geometrical features of the adopted restraints, and specifically on their influence in terms of global shear buckling response and actual normalized slenderness ratio (Figure 10(b)), as well as in the occurrence of possible local failure mechanisms leading the glass panels to failure. Careful consideration, consequently, should be paid in their design and verification under simple loading configurations as well as combined actions. In this sense, it is expected that the current research study could represent a valid theoretical background for the full implementation and development of standardized design methods for glass structures.

6. Conclusions

In this paper, the shear buckling response and actual resistance of glass walls has been assessed by means of extended Finite-Element (FE) numerical investigations and analytical methods derived from classical theory. Careful consideration has been paid, in particular, on the effect that actual restraints of practical use can have in terms of theoretical shear buckling resistance, fundamental buckling shape and ultimate buckling failure load. While standardized design methods are often implemented on the base of rather idealized boundary conditions, for glass structural elements and for construction materials in general, appropriate studies are required for a rational estimation of the actual behavior and resistance. In this research contribution, glass shear walls with (i) linear adhesive joints, (ii) bracing metal frames with interposed adhesive joints or (iii) point mechanical connectors have been explored, based on design concepts partly derived from past projects. Analytical fitting curves have been proposed for each one of the examined boundary conditions, in order to provide general applicability of classical buckling formulations in the rational calculation of the corresponding Euler's critical load. The possible extension of generalized design methods already in use for glass shear panels with ideal, continuous simply supports along the four edges has been then assessed for the aforementioned restraint configurations. As shown, a rather close agreement was found for all of them, due to the appropriate estimation of the restraints' effect. Finally, a practical case study has been also discussed, to further emphasize the role of restraints on the overall shear buckling performance of a given structural glass wall. It is thus expected, towards the implementation and calibration of standardized design rules, that the current exploratory research study could be further extended by means of full-scale experimental tests.

References

ABAQUS v.9.10 computer software, Dassault Systemes, Simulia (2010)

Amadio, C., Bedon, C.: An equivalent thickness for buckling verification of laminated glass panels under in-plane shear loads, Journal of Civil Engineering and Science, 2(3): 108-123 (2013)

Amadio, C., Bedon, C.: Effect of circumferential sealant joints and metal supporting frames on the buckling behavior of glass panels subjected to in-plane shear loads, Glass Structures & Engineering, published online, doi: 10.1007/s40940-015-0001-2 (2015)

Antolinc, D., Rajčić, V., Žarnić, R.: Analysis of hysteretic response of glass infilled wooden frames, Journal of Civil Engineering and Management; 20(4): 600-608 (2014)

Bedon, C., Amadio, C.: Buckling of flat laminated glass panels under in-plane compression or shear, Engineering Structures, 36: 185-197 (2012)

Bedon, C., Amadio, C.: Exploratory Finite-Element investigation and assessment of standardized design buckling criteria for two-side linear adhesively supported glass panels under in-plane shear loads, Engineering Structures, 106: 273-287 (2016a)

Bedon, C., Amadio, C.: Shear glass panels with point-fixed mechanical connections: Finite-Element numerical investigation and buckling design recommendations, Engineering Structures, 112: 233-244 (2016b)

Bennison, S.J., Jagota, A., Smith, C.A.: Fracture of glassy/poly(vinyl butyral) (Butacite®) laminates in biaxial flexure, Journal of the American Ceramic Society, 82(7): 1761 - 1770 (1999)

Behr, R.A.: Design of architectural glazing to resist earthquakes, Journal of Architectural Engineering, 12(3): 122-128 (2006)

Callewaert, D.: Stiffness of glass/ionomer laminates in structural applications. Ph.D. Dissertation; Ghent University, Faculty of Engineering and Architecture, ISBN 9789085784692 (2011)

CNR-DT 210/2013: Istruzioni per la progettazione, l'esecuzione ed il controllo di costruzioni con elementi strutturali di vetro. Technical Document; National Research Council, Rome, Italy

EN 572-2: 2004: Glass in buildings – Basic soda lime silicate glass products. CEN

Huveners, E.M.P., van Hervijnen, F., Soetens, F., Hofmeyer, H.: Glass panes acting as shear wall. Heron, Vol.52 (1/2), pp.5-29. http://alexandria.tue.nl/openaccess/Metis213320.pdf (2007)

Memari, A.M., Behr, R.A., Kremer, P.A.: Dynamic racking crescendo tests on architectural glass fitted with anchored pet film, Journal of Architectural Engineering, 10(1): 5-14 (2004)

Mocibob, D.: Glass panels under shear loading – Use of glass envelopes in building stabilization. PhD Thesis nr. 4185, EPFL Lausanne, Switzerland (2008)

Peterson, R.E.: Stress concentration design factors. John Wiley & Sons (1953)

Richter, C., Abeln, B., Geßler, A., Feldmann, M.: Structural steel-glass facade panels with multi-side bonding – Nonlinear stress-strain behaviour under complex loading situations, International Journal of Adhesion & Adhesives, 55: 18-28 (2014)

Timoshenko, S.P., Gere, J.M. Theory of Elastic Stability, 2nd Edition, McGraw-Hill, New York (1961)

Van Duser, A., Jagota, A., Bennison, S.J. Analysis of Glass/Polyvinyl Butyral (Butacite®) Laminates Subjected to Uniform Pressure, Journal of Engineering Mechanics, 125(4): 435-42 (1999)

Wellershoff, F.: Nutzung der Verglasung zur Aussteifung von Gebaüdehüllen. PhD Dissertation, RTWH Aachen, Shaker Verlag (2006)